



# IDENTIFICATION OF RUST DISEASES IN WHEAT CROP USING IMAGE ANALYSIS

RAVISANKAR MALLADI and RAJESH CHANDRA GOGINENI

Department of Computer  
Science and Engineering  
Gudlavalleru Engineering College (A)  
Gudlavalleru-521356, India  
Email: drmrsankar@gecgudlavallerumic.in

Department of Computer  
Science and Engineering  
SVR Engineering College  
Nandyal-518502, India  
Email: grajeshchandra@gmail.com

## Abstract

The future of the world is depending on present human health conditions that can be depending on our crop fields. Now-a-days all crop fields are being damaging by different types of diseases. In this article we have used some techniques of artificial intelligence and data mining by using field images for early identification of diseases to save the Wheat crop. We have implemented different types of comparison techniques for identifying the present position of a crop. A Mask RCNN model was retrained and used to see the spikes in concealing pictures and make cover for each spike, which is the purpose behind FHB distinguishing proof. In this manner, the display of the Mask RCNN model is key. If these limits are not set up, little spikes will be recollected affectionately and simply a piece of enormous spikes will be perceived.

## 1. Introduction

The future of the world explicitly depends upon the well-being of human. Thus humans' health plays a vital role. Their health status no doubt depend upon the staple food they consume. According to United Nations [2], the

---

2010 Mathematics Subject Classification: 68.

Keywords: Rust diseases, image comparison, DL Technique, RCNN Model and Mask RCNN Model.

Received November 20, 2020; Accepted December 18, 2020

current wheat supply is ample for global demand but it has to be increased keeping in mind the increasing rate of population which is expected to be nine billion by 2050.

The problem that the production faces is exacerbated by the diseases that are caused by rust pathogens. It is estimated that global annual loss to wheat rust pathogenesis close to five billion dollars per annum. Now the objective of this work is to identify the rust problem that wheat face at an early stage with the help of image processing. Early identification of disease will help the farmer to take the needed steps.





In the following figure we have shown the world wheat market from 2016 to November 2020. If we observe the production of wheat in entire world in million tonnes from 2016 to till date, the production is decreasing but supply and utilization is increasing.

**Table 1.** World's Wheat Market progress from 2016-2021.

<b>World Wheat Market</b>						
	2016-17	2017-18	2018-19	2019-20 (estimate)	2020-21 (Forecast)	Current 09-Nov-20
Million tones						
Production	763.5	761.6	732.9	732.9	764.8	762.7
Supply	1006.1	1026.3	1019.2	1033.2	1033.2	1038.5
Utilization	737.0	738.6	751.0	750.5	756.6	758.0
Trade	177.1	177.6	168.3	184.0	184.5	184.5
Ending Stocks	35.9	38.6	272.3	275.8	284.8	281.0
World stock to use ratio	19.8	21.9	36.2	36.4	36.4	36.4

Now-a-days the wheat fields are getting some diseases [1]. Those are Barley yellow dwarf, black Chaff, crown and root rot, leaf rust and tan spot. We are working on Leaf Rust diseases. We have collected some real time datasets related to wheat crop in India from online sources. By using the data sets we have designed new datasets. These datasets are divided into four categories those are named with Puccinia rust dataset, brown rust dataset and yellow dataset.

Some sample wheat leaf images are shown in the following figure 1.

Some Type of diseases	Images of wheat leaves
Puccinia rust wheat leaf	
Brown rust wheat leaf	
Yellow rust wheat leaf	
Healthy wheat leaf	

**Figure 1.** Comparison of diseases in wheat crop.

## 2. Analysis

In this article we have to do the comparison of different wheat leaves. By this comparison we can identify the rust disease. First of all we are taking the unknown leaf already we have four types of datasets. We are comparing new wheat leaf with rust brown rust wheat leaf by using image comparison techniques. By depending on the similarities between two leaves we can identify whether the new leaf has brown rust or not. If the similarity percentage is very high then we can realize that new wheat leaf has the brown rust disease. If we can't get any similarities between the new leaf with brown rust wheat leaf dataset then we can compare new leaf image with yellow rust wheat leaf. If any similarities are observed between new image with yellow rust wheat leaf image then we can decide the new leaf image has the yellow rust wheat leaf. Similarly we can check for Puccinia rust wheat leaf dataset where if we don't get any similarities then the new leaf has no disease this comparison goes on with image segmentation algorithms [5].

## 3. Classification

In the current morph physiological classification there are 10 significant kinds of delicate and hard wheat. Some of them are introduced as 2-5 subtypes. Let us presently consider the morphological qualities of parts of the

known morphophysiological types. Lamentably, the material accessible at the time didn't allow handling the information for all known morphophysiological types, nonetheless, the outcomes indicates that the mathematical qualities of shape have unmistakable explicit side effects that can be utilized both in the commonsense and the hypothetical viewpoints.

Above all else we are accepting a picture as an info picture. Next we are changing that 2D Digital picture over to dark scale picture. The accompanying code is helpful in getting a dark scale picture from unique picture.

```
L = imread ('rice.png')
```

```
Imshow (l(1:100, 1:100))% to show the first 100 pixels from the left top
```

```
Figure, imshow (l)% compare it with the entire image.
```

**Figure 1.** MAT lab code for generation of gray scale image.

Essentially like all pictures in all of our datasets we are producing lattice estimations of every single picture and putting it away in our informational indexes. At the point where we get another picture we create a framework estimations of that picture through its dark scale picture and contrasting the new lattice esteems and all network estimations of all pictures of all datasets on the off chance that any picture is coordinating the estimations of new picture grid esteems, at that point we need to presume that obscure picture's patient have the sickness that was distinguished by the dataset.

A definite objective of this investigation is to dependably distinguish ailing territories of individual spikes, which is where object recognition strategies are vital. The principal basic advance in this cycle is distinguishing the limits of the spikes and eliminating the foundation. In light of the DL strategy [6], He et al. proposed the Mask RCNN model, which can order objects, however it can likewise yield their layouts at the pixel level. It expands faster RCNN model by consolidating grouping, bouncing boxes, and cover age, which empowers example division. In particular, Mask RCNN has two primary advances. To start with, it examines a picture and creates various plausible anchor locales utilizing the district proposition organization to separate highlights. Second, the districts are assessed and arranged, which

creates bounding boxes and covers. Also, the “RoIAlign” layer was proposed to increase the segmentation accuracy, and loss function ( $L$ ) was defined as function (1).

$$L = L_{cls} + L_{box} + L_{mask} \quad (1)$$

Where  $L_{cls}$ ,  $L_{box}$ ,  $L_{max}$  represent the classification of bounding box and mask losses respectively.

In the current examination, Mask RCNN was executed utilizing Tensorflow API. The model was pretrained utilizing the COCO dataset [11], and just the last couple of layers were prepared and calibrated utilizing move learning. ResNet 50 and ResNet 101 [12] are two spine network alternatives. The previous one was utilized for this situation where given is its exactness and little preparing dataset. Cluster standardization was applied to forestall over fitting. The clump size was set to 2 since it requires just a limited quantity of memory. Five scales (i.e., 32, 64, 128, 256, and 512) and three proportions (i.e., 0.5, 1, and 2) were set for the anchors. In the event that the estimations of crossing point over the association proportion with the ground-truth jumping boxes were higher than 0.5, the anchors were viewed as accessible. Different boundaries were designed to the default setting.

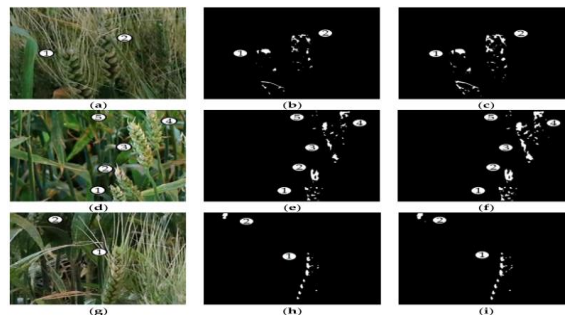


**Figure 2.** Examples of healthy and diseased spikes with three varieties (Wheaton, brown rust, and yellow rust) and shapes in the gray images: ( $a$ ,  $d$ ,  $g$ ). Color images of awned and awnless wheat varieties ( $b$ ,  $e$ ,  $h$ ). Gray images of number spike 1 in image  $a$ ,  $d$ , and  $g$  ( $c$ ,  $f$ ,  $i$ ). Gray images of spike 2.

We converted the color images to gray scale images and stored the data sets. After that by using DL Techniques and RCNN Model we are identifying

the rust diseases in given image we are marking it that is shown above image then we move on to image comparison between the images of each and every dataset.

First of all we have selected some unknown images related to the wheat crop then Convert that image to gray scale image by using equation 1. Already we have four types of datasets with the names yellow rust leaf dataset, puccinia rust leaf dataset brown rust leaf dataset. Later we have selected all images of one dataset and compare those with new unknown image by using  $K$ -means algorithm and Otsu's algorithm. If similarities are more than 70% then the leaf belongs to that dataset name thus we can confirm that the leaf has the rust of the name of that dataset.

#### 4. Results

The dark worth contrasts among unhealthy and solid pixels empower the discovery of the FHB-contaminated zones of each spike utilizing regular division calculations of AI. In this situation, the changed locale developing calculation was utilized to fragment the infected territories from the whole spike. The  $K$ -means and Otsu's calculations were additionally actualized to deal with the dark spike pictures utilized for the similar tests. After division, little potential zones were taken out, and close activity was applied to wipe out foundation commotion. The eventual outcomes are shown in Figures 12 and 13. In the current investigation,  $K$  was appointed to 4 thinking about the spatial goal of the pictures. Subsequently, the pixels in the dim pictures were classified into four classes, which incorporate the foundation, solid tissue, unhealthy tissue, and associated regions between the spikelets. The division results were troublesome on the grounds that the associated territories were ordinarily ordered accidentally (Figure 13b, e, h). In Figure 13c, *f*, *i*, the division exactness of Otsu's calculation was the least, and some non-unhealthy regions were inappropriately viewed as ailing zones. The district developing calculation could deal with the recently referenced issues and exhibit the ideal presentation in sectioning the infected regions. In spite of the fact that the covers may contain some non-spike pixels, the district developing calculation could fragment infected territories precisely. Besides this the infected regions were isolated into a few little areas, instead of just a gathering, as shown in Figure 12c, *f*, *i* in various shadings.

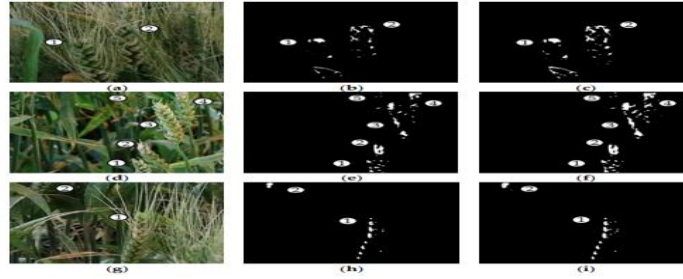


**Figure 3.** Segmentation results of the *K*-means algorithm and Otsu's algorithm: (a, d, g). Color images of awned and awn lesswheat varieties (b, e, h). FHB detection results of awned and awnless wheat varieties using the *K*-means algorithm (c, f, i). FHB detection results of awned and awnless wheat varieties using Otsu's algorithms.

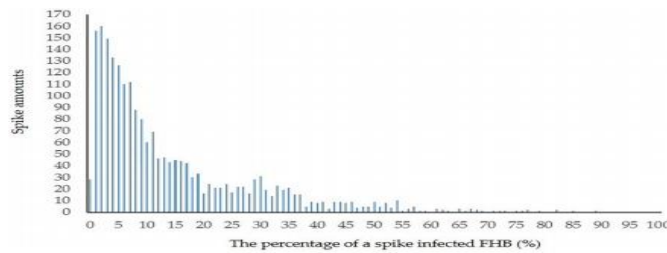


**Figure 4.** Number of spikes in each diseased percentage.

## 5. Conclusion

A Mask RCNN model was retrained and used to perceive the spikes in shading pictures and create veils for each spike, which is the reason for FHB identification. Subsequently, the exhibition of the Mask RCNN model is fundamental. In this examination, review, accuracy, and map were executed to survey the model. The retrained model had shown ideal execution in spike recognition (map is 0.9201). In any case, a few inquiries ought to be tended to and dissected further. To start with, the spikes speak to different directions in the shading pictures. Some neighboring spikes covered or their edges contacted, which made identifying each spike troublesome. This trouble is likewise the weakness of the Mask RCNN model. Second, the shading pictures contain whole spikes, yet additionally numerous halfway spikes. The tests indicated that the retrained model could identify some halfway spikes in

the shading pictures. Nonetheless, it was less compelling at perceiving spikes situated at the edges of a picture or those not in the profundity of field center. Ultimately, the setting of anchor boundaries which will influence the accuracy of spike identification. The spike sizes in shading pictures should be thought of. Hence, the anchor boundaries ought to be reliable with the spike sizes. In the event that these boundaries are not set up, little spikes will be remembered fondly and just a part of huge spikes will be recognized.

### References

- [1] A review of wheat diseases-a field perspective, *Molecular Plant Pathology* 19(6) DOI: 10.1111/mpp.12618, Melania Figueroa, Kim Hammond-Kosack, Peter Scott Solomon (2017).
- [2] World's food and agriculture organization of United Nations, <http://www.fao.org/worldfoodsituation/csdb/en/>.
- [3] Online data from <http://github.com/jbrownlee/datasets/blob/master/wheat-crops.csv>
- [4] T .V. Vishal, S. Srinidhi, S. Srividhya, K. Sri Vishnu Kumar and R. Swathika, A Survey and Comparison of Artificial Intelligence Techniques for Image Classification and Their Applications, *International Journal of Science and Research* 5(4) April (2016), 187-193.
- [5] Daniel Paternain, Mikel Galar, Aranzazu Jurio and Edurne Barrenechea, A new algorithm for color image comparison based on similarity measures, 8th Conference of the European Society for Fuzzy Logic and Technology (EUSFLAT 2013).
- [6] Ruicheng Qiu, Ce Yang, Ali Moghimi, Man Zhang, Brian J. Steffenson and Cory D. Hirsch, Detection of Fusarium head blight in wheat using a deep neural network and color imaging, *Remote Sens.* (2019) 11, 2658; doi:10.3390/rs11222658.
- [7] S. Madec, X. Jin, H. Lu, B. De Solan, S. Liu, F. Duyme, E. Heritier and F. Baret, Ear density estimation from high resolution RGB imagery using deep learning technique, *Agric. For. Meteorol.* 264 (2019), 225-234.
- [8] S. P. Mohanty, D. P. Hughes and M. Salathé, Using deep learning for image-based plant disease detection, *Front. Plant Sci.* 7 (2016), 14-19.
- [9] H. Buerstmayr, T. Ban and J. A. Anderson, QTL mapping and marker-assisted selection for Fusarium head blight resistance in wheat: A review, *Plant Breed.* 128 (2009), 1-26.
- [10] K. He, G. Gkioxari, P. Dollár and R. Girshick, Mask R-CNN, arXiv 2017, arXiv:170306870.
- [11] T. Y. Lin, M. Maire, S. Belongie, J. Hays, P. Perona, D. Ramanan, P. Dollár and C. L. Zitnick, Microsoft COCO: Common objects in context. In *Computer Vision-ECCV 2014*; D. Fleet, T. Pajdla, B. Schiele, T. Tuytelaars, Eds.; Springer International Publishing, Cham, Switzerland (2014), 740-755.



- [12] K. He, X. Zhang, S. Ren and J. Sun, Deep residual learning for image recognition, In Proceedings of the European Conference on Computer Vision, Amsterdam, the Netherlands, 8-16 October (2016), 770-778.
- [13] B. C. Russell, A. Torralba, K. P. Murphy and W. T. Freeman, Label Me: A database and web-based tool for image annotation, *Int. J. Comput. Vis.* 77 (2008), 157-173.
- [14] R. Qiu, C. Yang, A. Moghimi, J. Anderson, B. J. Steffenson and P. Marchetto, Detection of Fusarium Head Blight in Small Grains Using Hyper spectral Imaging, National Fusarium Head Blight Forum: Saint Louis, MO, USA, (2018), 32-37.
- [15] Github, Available online: <https://github.com/ZQPei/Seeded-Region-Growing-Algorithm> (accessed on 10 September 2019).